# Practical evaluation of carrier sensing for a LoRa wildlife monitoring network

Morgan O'Kennedy*, Thomas Niesler†, Riaan Wolhuter†, Nathalie Mitton‡
*† Dept. of Electrical and Electronic Engineering, University of Stellenbosch, South Africa, ‡Inria, France
*morgan.okennedy@gmail.com, †{trn, wolhuter}@sun.ac.za, ‡nathalie.mitton@inria.fr

***Abstract*—We consider the technique of carrier sensing for application in a LoRa mesh network aimed at wildlife monitoring. A key challenge in this application is to limit collisions in order to increase the channel capacity. Since CSMA is very rarely applied in LoRa-based networks, our goal is to determine its practical viability. We evaluate the LoRa Channel Activity Detection (CAD) mechanism under laboratory and field conditions. Our results show that both preamble and payload symbols are detectable even at distances exceeding 4 km. Detecting LoRa preamble symbols had a SNR advantage of between 1 and 2 dB over payload symbols. Furthermore, we find that by taking at least 8 consecutive CAD measurements during payload frame time, a clear channel assessment (CCA) comparable to the LoRa frame reception rate can be achieved between two nodes.**

***Index Terms*—LoRa, MAC, CSMA, CAD, mesh network, WSN**

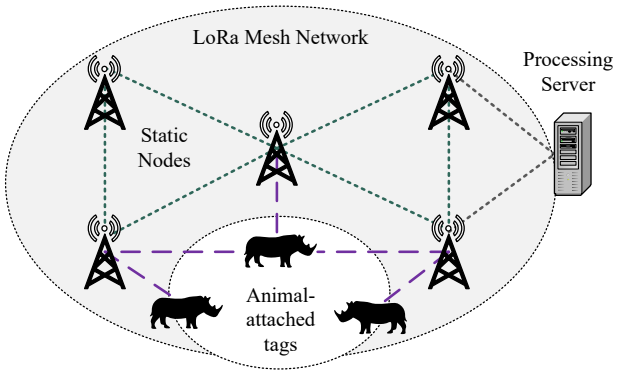


Fig. 1. A wildlife monitoring mesh network.

## I. Introduction

With the rapid decrease in the populations of threatened animal species, the ability to remotely monitor wildlife in their natural habitat has become a necessity. In South Africa, the population of rhinoceros is under severe threat due to illegal poaching for their horns. Over the period 2013–2018, approximately 1000 rhinos were killed each year in national parks by poachers [1]. These parks are in remote locations, often with poor infrastructure and no cellular network coverage. They often cover large areas, with the largest, the Kruger National Park, covering more than 20 000 square kilometers. Consequently, current technological anti-poaching strategies have proved to be largely ineffective.

We have developed prototype animal-borne biotelemetry sensor tags with the aim of detecting abnormal behavioral patterns that can alert a proactive response [1]. A major challenge remains the reliable gathering of data in a cost-effective manner over the vast, remote areas that form the habitat of the animals under threat. In [2] the authors have proposed a dual radio architecture using both Bluetooth Low Energy (BLE) and LoRa modules, but the targeted parks are either small or the existing infrastructure and terrain allows for single-hop LoRaWAN communication. In [3], the authors have evaluated several low-cost radio transceiver modules and found that LoRa-capable devices outperformed similar candidates for a practical wildlife monitoring wireless sensor network. A prototype network with Ad hoc On-Demand Distance Vector (AODV) routing was also developed to demonstrate the feasibility of a LoRa-based mesh network (Fig. 1).

In a LoRa network, channel access is typically attained by a random-access method, similar to ALOHA, where collisions are not explicitly avoided [4]. Such networks have a well-known channel capacity limitation of roughly 0.18 packets per packet-time [5]. This limitation might have a significant performance impact on our intended network for a number of reasons. Firstly, our application would benefit from maximizing the communication range by using very low data rates. Therefore, the Time-On-Air (ToA) per data transmission can be several seconds. Secondly, our low-cost static node hardware implementation utilises only a single radio module. This implies a network-wide default channel on which all nodes communicate. Thirdly, static nodes will further fill the channel occupancy by forwarding data to a central data processing server. Finally, our animal sensor tags are designed with the utmost frugality in terms of power consumption. As a result, regular clock synchronization by means of GPS or network packets is not feasible for most network nodes. We therefore require a protocol that will allow asynchronous communication in order to support infrequent tag wake-up periods and that does not depend on accurate time synchronization for each initiated transmission.

Several studies have analyzed the potential benefit of Carrier-Sense Multiple Access (CSMA) for LoRa-based networks [6]–[8]. However, there is very little information on the practical performance of LoRa CSMA over long distances. Therefore, in this paper, we propose a method with which to evaluate the LoRa CSMA mechanism and to determine its viability for a Medium Access Protocol (MAC) design that aims to decrease collisions and thus increase channel capacity.

ISBN 978-3-903176-28-7©2020

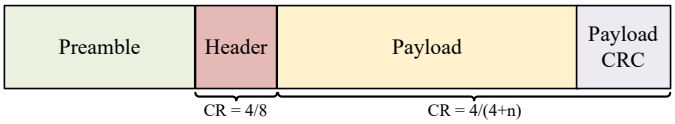


Fig. 2. The LoRa physcial frame structure. The payload Coding Rate (CR) parameter has a user selectable range {4/5, 4/6, 4/7, 4/8}.

## II. Background

### A. LoRa and LoRaWAN

LoRa is a proprietary spread spectrum modulation scheme [9]. It implements a variation of chirp spread spectrum that offers increased communication range in exchange for a low data rate. The data rate for a given channel bandwidth (BW) is determined by choosing a spreading factor (SF) parameter where SF $\in \{7, \ldots, 12\}$. The higher the SF, the more BW is used per symbol, resulting in a lower data rate and increased receiver sensitivity. The symbol period is given in [9] by $T_{sym} = 2^{\mathrm{SF}}/BW$. The LoRa physical frame structure has four parts: a preamble (which is used for receiver synchronization), an optional frame header (which consists of frame parameters), a payload and finally an optional payload CRC (Fig. 2).

LoRaWAN is an open standard MAC protocol that utilizes LoRa modulation as the physical layer [10]. It acts as a star-topology networking protocol for managing communication between end-devices and internet gateways. The gateway is then responsible for routing packets to a central network server. Readers are referred to [9] and [10] for a more comprehensive description. Since it is both impractical and uneconomical to provide sufficient internet gateways in our largest parks, this study focusses on LoRa nodes that do not necessarily rely on LoRaWAN.

### B. CSMA on LoRa-based networks

It has been demonstrated by simulation that CSMA can be effectively applied to LoRa networks with a high node count [6]–[8]. A practical experiment with 50 nodes was conducted in [11] to determine the effectiveness of CSMA as a collision avoidance mechanism. This work showed a $\sim$20% higher packet reception rate when using inter-packet delays of 2–5 seconds and a payload size of 8 bytes. Unfortunately, neither the experimental node distances nor the radio conditions are described.

A practical evaluation of CSMA for long LoRa payloads between 2 nodes was performed in [12]. First, a protocol was adapted from the IEEE 802.11 Distributed Coordinated Function's (DCF) basic CSMA mechanism. It was found that this mechanism becomes unreliable with increased range which impacts negatively in a real-world deployment. For example, the technique was found to be effective up to 1 km in non-line-of-sight conditions and only up to 400m in dense vegetation. An extended DCF Inter-Frame Space (DIFS) was suggested and defined as the maximum transmission ToA in which periodic carrier detection was performed. However, the radio conditions for which the proposed mechanism is expected to become unreliable were not described. Finally, both [11] and [12] find that the CSMA mechanism can occasionally successfully detect the payload part of a frame. However, this is an unspecified functionality of the radio module [13] and no information is available on the limitations of this unexpected behaviour.

Apart from the studies mentioned above, we are not aware of other practical CSMA implementations on LoRa-based networks. For instance, LoRaWAN does not apply CSMA in its design.

## III. The carrier-sense multiple access mechanism

### A. LoRa physical CSMA capabilities

LoRa radio modules can detect channel activity using two distinct mechanisms. First, the Received Signal Strength Indicator (RSSI) can be monitored. The RSSI level is a relative measure of the total RF energy a node receives at its antenna, regardless of whether it is a LoRa signal or not. Although this approach can be suitable when the signal is strong, the LoRa module is able to demodulate transmissions below the RF noise floor due to its inherent processing gain (Tab. I). Thus, for our intended long-range application, this mechanism is not ideal.

TABLE I
Range of spreading factors with associated periods and reception sensitivity at 125 kHz BW [9], [13].

| Spreading Factor | Symbol Period (ms) | Measured CAD duration (symbols) | Demodulator cut-off SNR (dB) |
|---|---|---|---|
| 7 | 1.024 | 2.40 | - 7.5 |
| 8 | 2.048 | 2.01 | -10.0 |
| 9 | 4.096 | 1.86 | -12.5 |
| 10 | 8.192 | 1.83 | -15.0 |
| 11 | 16.384 | 1.84 | -17.5 |
| 12 | 32.768 | 1.86 | -20.0 |

The second mechanism is the so-called "Channel Activity Detection" (CAD) and is designed specifically to detect LoRa preamble signals (chirps) below the noise floor. This function is activated by placing the radio module into a specific CAD-mode in which it captures radio samples for about one symbol period from the selected channel [13]. The modem then searches for a correlation between the captured samples and the ideal chirp waveform for the selected spreading factor (SF). If the correlation is strong, a "CAD detected" interrupt is generated. Otherwise, a "CAD done" interrupt is raised[1]. The result of a CAD measurement is thus a single binary value. The total duration of this operation is about 2 symbol periods (Tab. I) and during this time the receiver is not able to receive packets normally. The CAD-technique is the recommended mechanism employed by the LoRa module for a CSMA clear channel assessment (CCA) and is the focus of the remainder of this paper. A major drawback of its use is the stated inability to detect the payload part of the LoRa frame[2]. Currently, it is also unclear under which radio conditions this mechanism becomes unreliable. Therefore, the key aim in Section IV is to discover

the limitations of the CAD mechanism more precisely in order to allow informed decisions in our MAC protocol design.

### B. CSMA/CA implementation in IEEE 802.11

The IEEE 802.11 DCF standard is widely adopted as the MAC-layer for WLAN and wireless ad-hoc networks. It specifies a physical and virtual method for performing CSMA. In order to alleviate the well-known hidden terminal problem, an optional "virtual carrier sensing" mechanism is also defined. It is usually configured to be used for frames exceeding a specified size. A request-to-send/clear-to-send (RTS/CTS) handshake is incorporated to reserve access to the channel.

### C. A combined CSMA implementation for a LoRa multi-hop wildlife network

In the previous work discussed in Section II-B, CSMA was considered only for single-hop LoRa communication. Correspondingly, only physical carrier sensing was evaluated. Our envisioned application in a multi-hop scenario is expected to suffer from hidden terminals which negatively impact on the network's performance. For our complete MAC-layer implementation, we therefore propose physical carrier sensing using a method similar to [12] but applied in conjunction with the RTS/CTS control frames. In addition to alleviating the hidden terminal problem, the control frames are also used to select the closest static node to which the data frames are sent. Additionally, data payloads can be concatenated to form longer payloads that are only sent when network coverage is detected by a CTS frame. These methods are chosen specifically to reduce energy consumption on the animal-borne tag by minimising data packet loss when network coverage is sparse. However, the number of CADs required to accurately perform a CCA is currently unknown. According to our knowledge, no study has accurately measured this requirement. As multiple CADs imply considerable delays, this parameter will ultimately help determine the minimum SIFS/DIFS duration for our LoRa-based CSMA MAC implementations.

## IV. Experimental setup

### A. Node hardware configuration

We have used the Nucleo-L073RZ development board as the main processing unit for all nodes in our experiments. The Adafruit RFM96W 433MHz LoRa module was configured as the radio transceiver (Tab. II). The nodes were supplied with grid power in the laboratory experiments. In the outdoors, however, power was provided by 4W solar panels and a 10Ah Li-ion battery pack.

### B. Evaluation of CAD in the laboratory

A laboratory test was conducted to simulate the radio module's carrier sensing behaviour under poor radio conditions.

[1]Only the SX127x family of LoRa radio modules are considered here.

[2]The most recent SX126x radio modules claim to support CAD-detection in the physical frame payload. Due to the unavailability of such integrated modules in the 433MHz band at the time of writing, this was not evaluated.

TABLE II
RFM96W module configuration.

| Module Parameter | Value |
|---|---|
| RF Frequency | 433.175 MHz |
| Bandwidth | 125 kHz |
| Preamble Symbols | 8 |
| Coding Rate | 4/5 |
| Spreading Factor | {7, 9, 11} |

The objective was to find the precise limitations of the CAD mechanism provided by the RFM96W.

We made use of two RF step attenuators to accurately control the RF power (-121–0 dB) transmitted from a master node to several receiver nodes. Before starting the measurements, the master node transmission was attenuated to the threshold at which the receiver could still successfully decode the frame. The receiver nodes were placed inside a RF shielded enclosure to ensure that no spurious emissions would influence the measurements. The attenuated master node signal was then fed to an antenna inside the enclosure. The following CAD measurement procedure was then performed for SFs 7, 9 and 11:

- The master would set its RF power to maximum $P_{max}$. It then sends a notification to all listening nodes informing them that a CAD measurement transmission is about to begin.
- When a node receives the notification, it waits for a SIFS duration after which it performs 20 consecutive CAD measurements. The master node is configured to start another 8-byte transmission containing random data at exactly the same time as the first CAD measurement.
- The listening node saves the result of each CAD measurement, together with the RSSI and SNR of the measurement notification. These results are sent back to the master node at coordinated intervals.
- The master node then reduces its transmission power by 1 dBm and the process repeats until $P_{min}$. The transmission power is then restored to $P_{max}$ and the full process is repeated.

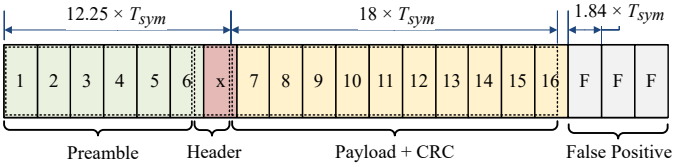


Fig. 3. The structure of the 20 consecutive CAD measurements, showing the near-perfect synchronization for a 8-byte payload at SF11. A total of 16 successfull detections can be performed.

With no RF attenuation, the CAD measurements were observed to always successfully detect the full 8-byte physical frame sent by the master, with the exception of the measurement during the frame header (Fig. 3). This measurement could never detect the channel as occupied and was consequently discarded in the calculation of the CAD error rates.

The preamble and payload consist of 6 and 10 measurements respectively, except in the case of SF7, where the preamble consists of 5 measurements. Three additional measurements after the completion of the transmission were used to calculate the CAD false positive rate. Attenuated transmissions resulted in a lower probability of successful CADs during both parts of the frame. To gain reliable averages, the experiment was repeated to obtain approximately 35 000 frame measurements for each SF. A second experiment considered only CAD within the payload part of the physical frame. This was achieved by including appropriate delays between transmitter and receiver. It was observed that the results correspond with simply discarding all preamble measurements from the first experiment.

### C. Evaluation of CAD in the outdoors

To validate our laboratory measurement results in a real-world environment, we performed the same procedure described in the previous section in an outdoor environment. A master node was installed on the roof of the Department's building at an estimated height of 22m above ground level. Secondary field nodes were placed on farmlands approximately 4 km away. This scenario is comparable to the envisioned deployment of a sink node in a national park rest camp and a static node on a nearby hill. Since the CAD measurement results are sent back to the master node, they can be easily collected and analysed. The procedure was run over multiple days to capture 60 000 measurements per node.

## V. Experimental Results

### A. Results of the laboratory experiments

The CAD error rates versus SNR at 3 different SFs are shown in Figure 4. The SNR shown is the value reported by the LoRa radio module as described in Section IV-B. For each SF dataset, all CAD measurements were grouped by SNR. CADs measured during the frame preamble and payload are calculated separately. The average CAD error rate (CER) was calculated per SNR group as follows:

$$\mathrm{CER}_{snr} = 1 - \frac{1}{n \cdot m} \sum_{i=1}^{m} \sum_{j=1}^{n} \mathrm{CAD}_{i,j,snr} \tag{1}$$

where $m$ is the total number of CAD measurements for a particular SNR and $n$ the number of preamble or payload measurements per frame (as shown in Fig. 3). The CER considers only the failure to detect the channel activity (false negatives). The CAD false positive rate, i.e. the detection of activity when no transmission was underway, was measured as below $1 \times 10^{-4}$ and therefore not shown. The cut-off SNR associated with each spreading factor (Tab. II) is shown in grey. It is observed that the CER resemble bit error rate (BER) curves. At a preamble CER of 0.5, the corresponding SNR is found to be at 1.5, 1.75 and 2.5 dB above the cut-off SNR for SF7, SF9 and SF11 respectively. Contrary to the indications in the manufacturer's official datasheet, the LoRa module was found to be able to detect channel activity during the payload

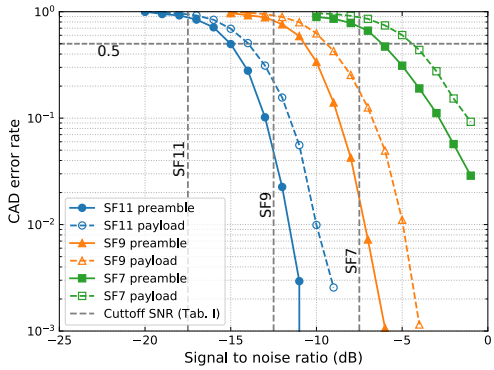


Fig. 4. Laboratory-measured CAD error rates (CER) for measurements at SF7, SF9 and SF11.

part of the frame, but at a 1 – 2 dB reduced SNR sensitivity relative to the preamble.

To compensate for this reduced sensitivity during the payload, we considered the effect of performing multiple consecutive CADs as suggested in Section IV. The cumulative result of these multiple CADs is defined as the CCA. For each frame, the logical OR of the $n$ collected measurements was determined. Because of the binary nature of these values, this operation can be expressed as $\max(\mathrm{CAD}_1, \mathrm{CAD}_2, \ldots, \mathrm{CAD}_n)$ so that the average CCA error rate (CCER) is given by:

$$\mathrm{CCER}_{snr} = 1 - \frac{1}{m} \sum_{i=1}^{m} \max_{j=1,\ldots,n} (\mathrm{CAD}_{j,i,snr}) \tag{2}$$

Due to the absence of comparable results from similar experiments in the literature, a theoretical estimate of the LoRa bit error probability ($P_b$) was required. Several such estimates have been presented, but the one derived in [14] was found to coincide most closely with our preliminary test observations. Equation (3) was derived using a simplified decoder implementation under an additive white Gaussian noise (AWGN) channel. Assuming no forward error correction, the symbol error probability ($P_s$) and frame error probability ($P_f$) are given by Equations (4) and (5),

$$P_b = Q\left(\frac{\log_{12}(\mathrm{SF})}{\sqrt{2}} \cdot \frac{E_b}{N_0}\right) \tag{3}$$

$$P_s = 1 - (1 - P_b)^{\mathrm{SF}} \tag{4}$$

$$P_f = 1 - (1 - P_s)^k \tag{5}$$

where $Q(x)$ is the $Q$-function, $E_b/N_0$ is the energy per bit to noise spectral density ratio and $k$ is the number of payload symbols per frame, e.g. $k = 18$ for an 8-byte payload at SF11.

Figure 5a shows the SF11 CCER when including the entire preamble as well as when $n \in \{1, 2, 4, 6, 8\}$ for payload measurements. The frame error probability using Equation (5) is shown for comparison (in grey). As might be expected, the lowest CCA is obtained when the entire preamble is consecutively measured (in black). However, it is also observed that, for 8 payload CAD measurements (in red), the CCA reliability is almost as good. Using still fewer CADs results in

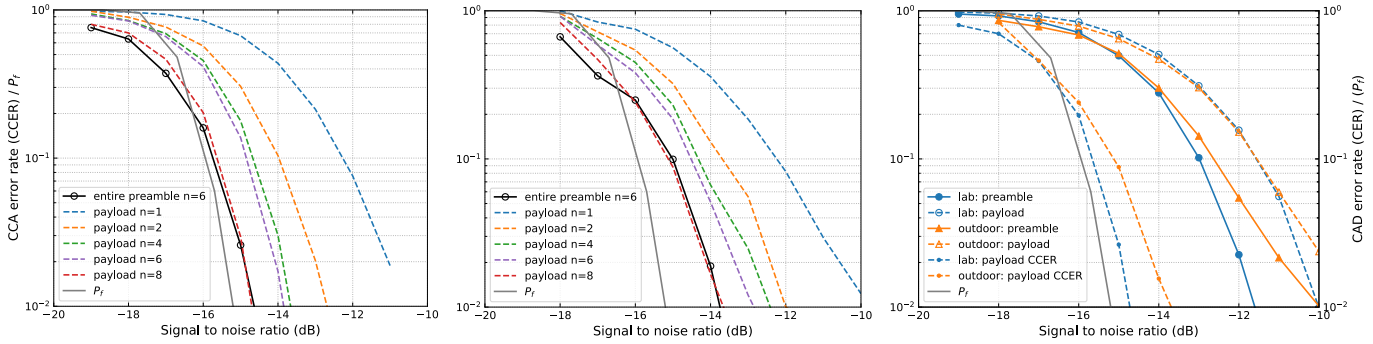


(a) Laboratory-measured CCA error rates. (b) Outdoor-measured CCA error rates. (c) Comparison of laboratory and outdoor-measured error rates.

Fig. 5. CCA error rates (CCER) when measuring the entire preamble ($n = 6$) as well as when taking $n$ consecutive payload measurements at SF11. In (c), the payload CCA consists of 10 CADs to measure the entire payload.

a sensitivity of up to 4 dB below this achievable rate. Fig. 5a also shows that, by applying 8 CADs, the CCA sensitivity is comparable to the theoretical frame error probability ($P_f$) predicted by Equation (5).

### *B. Results of the outdoor experiments*

Figure 5b shows the CCER for the entire preamble and n payload measurements for the outdoor dataset. The CCER has a slightly wider deviation from the frame error probability than the laboratory measurements. However, our finding that 8 payload CADs are needed to achieve a CCA accuracy comparable to that achieved when measuring the entire preamble still holds. Consequently, to minimize the probability of detecting a false clear channel, a reliable MAC protocol should include at least 8 consecutive CAD measurements for its CCA.

Figure 5c compares laboratory and outdoor experimental results for one particular field node. Similar results were obtained for the other field nodes. We observe a good agreement between the indoor and outdoor results for CAD error rates above $10^{-1}$. This indicates that the mechanism is viable even over the extended range of 4 km. The deviation observed at lower error rates was found to be due to noise introduced by the solar charger circuitry.

## VI. Conclusion

We have evaluated the LoRa CAD technique to assess its viability as a physical CSMA mechanism for a wildlife monitoring network. Indoor and outdoor experimental evaluation established that it is feasible to detect both the preamble and the payload part of the LoRa physical frame using LoRa CAD, even at distances exceeding 4 km. Applying CAD to the LoRa preamble symbols had an average SNR advantage of about 2 dB over its application to payload symbols. We also conclude that by taking 8 or more consecutive CAD measurements, a CCA sensitivity comparable to the LoRa frame reception rate can be achieved. In environments with high radio frequency interference, it is expected that more CAD measurements may be required to maintain this reliability. This requirement, together with its associated delays, should be considered when implementing a LoRa-based CSMA protocol where reliable carrier sensing is essential over long distances. The development of a complete MAC protocol to incorporate this mechanism is part of our ongoing work.

## References


[1] S. P. le Roux, R. Wolhuter, N. Stevens and T. Niesler, "Reduced Energy and Memory Requirements by On-Board Behavior Classification for Animal-Borne Sensor Applications," IEEE Sensors Journal, vol. 18, no. 10, pp. 4261–4268, 2018.

[2] E. D. Ayele, N. Meratnia and P. J. M. Havinga, "Towards a New Opportunistic IoT Network Architecture for Wildlife Monitoring System," 2018 9th IFIP International Conference on New Technologies, Mobility and Security (NTMS), Paris, pp. 1–5, 2018.

[3] J. Wotherspoon, R. Wolhuter and T. Niesler, "Choosing an integrated radio-frequency module for a wildlife monitoring wireless sensor network," 2017 IEEE AFRICON, Cape Town, pp. 314–319, 2017.

[4] A. Augustin, J. Yi, T. Clausen, and W. M. Townsley,"A Study of LoRa: Long Range & Low Power Networks for the Internet of Things," Sensors, vol. 16, no. 9, Sept. 2016.

[5] D. Magrin, M. Centenaro and L. Vangelista, "Performance evaluation of LoRa networks in a smart city scenario," 2017 IEEE International Conference on Communications (ICC), Paris, pp. 1–7, 2017.

[6] T. To and A. Duda, "Simulation of LoRa in NS-3: Improving LoRa Performance with CSMA," 2018 IEEE International Conference on Communications (ICC), Kansas City, MO, pp. 1–7, 2018.

[7] M. O. Farooq and D. Pesch, "A Search into a Suitable Channel Access Control Protocol for LoRa-Based Networks," 2018 IEEE 43rd Conference on Local Computer Networks (LCN), Chicago, IL, USA, pp. 283–286, 2018.

[8] S. Ahsan, S. A. Hassan, A. Adeel and H. K. Qureshi, "Improving Channel Utilization of LoRaWAN by using Novel Channel Access Mechanism," 2019 15th International Wireless Communications & Mobile Computing Conference (IWCMC), Tangier, Morocco, pp. 1656–1661, 2019.

[9] Semtech Corporation. "LoRa Modulation Basics - Application Note 1200.22," Revision 2, Semtech Corporation: CA, USA, 2015.

[10] LoRa Alliance, "LoRaWAN 1.1 Specification," LoRa Alliance: Beaverton, OR, USA, 2017.

[11] J. C. Liando, A. Gamage, A. W. Tengourtius, and M. Li, "Known and unknown facts of LoRa: Experiences from a large-scale measurement study," ACM Transactions on Sensor Networks (TOSN), vol. 15, no. 2, p. 16, 2019.

[12] C. Pham, "Investigating and experimenting CSMA channel access mechanisms for LoRa IoT networks," 2018 IEEE Wireless Communications and Networking Conference (WCNC), Barcelona, pp. 1–6, 2018.

[13] Hope RF Microelectronics, "RFM95/96/97/98(W) - Low Power Long Range Transceiver Module," v1.0; Hope RF Microelectronics: Shenzhen, China, 2016.

[14] B. Reynders, W. Meert and S. Pollin, "Range and coexistence analysis of long range unlicensed communication," 2016 23rd International Conference on Telecommunications (ICT), Thessaloniki, pp. 1–6, 2016.